Acta Crystallographica Section B
Structural Science
ISSN 0108-7681

Determination of the structure of the violet pigment $C_{22}H_{12}Cl_2N_6O_4$ from a non-indexed X-ray powder diagram

Martin U. Schmidt,[a]* Martin Ermrich[b] and Robert E. Dinnebier[c]

[a]Institute for Inorganic and Analytical Chemistry, J. W. Goethe University, Marie-Curie-Str. 11, D-60439 Frankfurt am Main, Germany, [b]X-ray Laboratory Dr Ermrich, Am Kandelborn 7, D-64354 Reinheim (Odenwald), Germany, and [c]Max-Planck Institute for Solid State Research, Heisenbergstrasse 1, D-70569 Stuttgart, Germany

Correspondence e-mail: m.schmidt@chemie.uni-frankfurt.de

Received 7 June 2004
Accepted 25 October 2004

The violet pigment methylbenzimidazolonodioxazine, $C_{22}H_{12}Cl_2N_6O_4$ (systematic name: 6,14-dichloro-3,11-dimethyl-1,3,9,11-tetrahydro-5,13-dioxa-7,15-diazadiimidazo-[4,5-*b*:4′,5′-*m*]pentacene-2,10-dione), shows an X-ray powder diagram consisting of only *ca* 12 broad peaks. Indexing was not possible. The structure was solved by global lattice energy minimizations. The program *CRYSCA* [Schmidt & Kalkhof (1999), *CRYSCA*. Clariant GmbH, Pigments Research, Frankfurt am Main, Germany] was used to predict the possible crystal structures in different space groups. By comparing simulated and experimental powder diagrams, the correct structure was identified among the predicted structures. Owing to the low quality of the experimental powder diagram the Rietveld refinements gave no distinctive results and it was difficult to prove the correctness of the crystal structure. Finally, the structure was confirmed to be correct by refining the crystal structure of an isostructural mixed crystal having a better X-ray powder diagram. The compound crystallizes in $P\bar{1}$, $Z = 1$. The crystal structure consists of a very dense packing of molecules, which are connected by hydrogen bridges of the type N—H···O═C. This packing explains the observed insolubility. The work shows that crystal structures of molecular compounds may be solved by lattice energy minimization from diffraction data of limited quality, even when indexing is not possible.

1. Introduction

In recent years methods for the determination of crystal structures from X-ray powder data have progressed considerably. This holds for the 'classical' approaches such as direct methods (Cascarano *et al.*, 1992; Altomare *et al.*, 1999; Chan *et al.*, 1999) or Patterson methods (Wagner *et al.*, 2001; Lasocha *et al.*, 2001), as well as for the more recent methods such as the real-space methods (see *e.g.* Reck *et al.*, 1988; Hammond *et al.*, 1996; Chernyshev & Schenk, 1998; David *et al.*, 1998; Engel *et al.*, 1999; Putz *et al.*, 1999; Dinnebier *et al.*, 2000; MacLean *et al.*, 2000; Cheung *et al.*, 2002; for reviews see: Harris & Tremayne, 1996; Harris *et al.*, 2001).

A fundamental requirement of all these methods is the knowledge of the lattice parameters in advance; *i.e.* the X-ray powder pattern must be indexed. However, many X-ray powder diagrams cannot in fact be indexed. The reasons include too small a particle size (*e.g.* far below 100 nm) and lattice strain, both of which result in severe line broadening and hinder the separation of overlapping peaks, so that the accurate peak positions cannot be determined (Shirley, 1980). If the sample is not chemically pure, or contains a mixture of crystal phases, additional lines disturb the indexing procedure.

Sometimes, the indexing programs may fail, even for high-resolution data, *e.g.* if the parameters are set inadequately. Furthermore, the user may consider a proposed indexing as 'unlikely', although it is the correct one.

If the X-ray powder diagram cannot be indexed, only three methods remain for solving the crystal structure:

(i) The crystal structure is solved by intuition, model building or comparison with other known structures (a considerable number of crystal structures are solved this way).

(ii) The crystal structure is solved by other experimental methods, *e.g.* by electron diffraction (Dorset, 1996; Voigt-Martin *et al.*, 1999; Kolb & Matveeva, 2003).

(iii) Independent of the X-ray powder diagram, the possible crystal structures are calculated (predicted) by global lattice energy minimization, *i.e.* by searching the energetically most favorable solid-state packings of a given molecule. For all energetically favorable structures, the X-ray powder diagrams are simulated and compared with the experimental X-ray powder diagram to find out which of the possible crystal structures corresponds to the given crystal modification. Finally, the structure is refined by Rietveld methods (Rietveld, 1967, 1969).

The third approach – a combination of global lattice energy minimization with subsequent Rietveld refinement – was repeatedly suggested in the literature (Louër *et al.*, 1995; Fagan *et al.*, 1995; Gavezzotti & Filippini, 1996; Bond & Jones, 2002); but to our knowledge, there is only one example so far (Erk, 2002) where a crystal structure was fully solved from only low-quality X-ray powder diffraction data, without prior knowledge of the lattice parameters.

We now used this approach to solve the crystal structure of $C_{22}H_{12}Cl_2N_6O_4$ (see Fig. 1).

The lattice energy minimization requires knowledge of the (approximate) molecular geometry as input. For flexible molecules the corresponding intramolecular degrees of freedom also have to be considered. If no information about the lattice parameters and space groups is available, the statistically most common space groups or those space groups which are popular for compounds of the same class are tested, and the lattice parameters are optimized together with the position and orientation of the molecules with their intramolecular degrees of freedom (an overview on methods and programs is given by Verwer & Leusen, 1998). The resulting packings are sorted according to energy. The energetically most favorable structures are regarded as possible polymorphic forms of the compound. Three blind tests (Lommerse *et al.*, 2000; Motherwell *et al.*, 2002, 2005) have shown that, generally, the geometric accuracy of the predicted crystal structures is quite good (*ca* 0.1–0.2 Å), whereas the energetic accuracy is less so: in most cases the experimental crystal structure was found in the list of predicted structures, but sometimes with an energy considerably above that of the lowest-energy structure, depending on the compound and the force field used (Lommerse *et al.*, 2000; Motherwell *et al.*, 2002, 2005). On the other hand, an accurate energy ranking is not crucial for solving a crystal structure from X-ray powder data, as long as the structure is contained in the list of predicted structures and the geometry is good enough for the powder diagram to be recognized as being similar to the experimental one. (This can be a problem since powder diagrams are very sensitive to small changes in the packing and in the molecular conformation. Furthermore, as long as the lattice parameters are not quite correct, the observed peak positions do not match the calculated positions.) The geometrical accuracy of the calculated structures is generally sufficient to serve as the starting point for a Rietveld refinement.

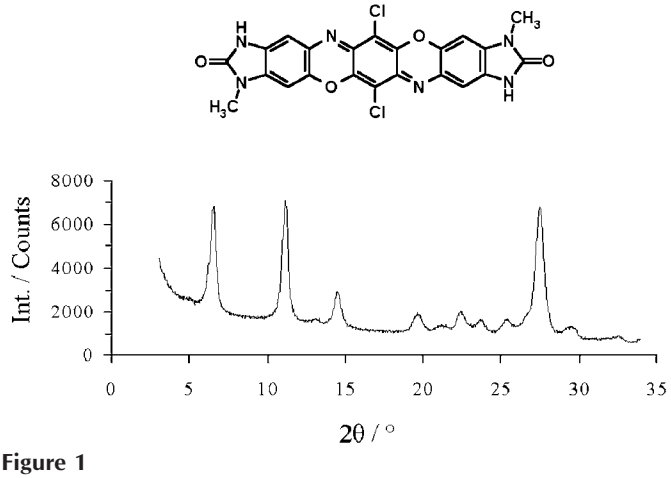

Figure 1
The investigated compound, $C_{22}H_{12}Cl_2N_6O_4$(1*a*), and the X-ray powder diagram used to solve the structure.

Compound (1*a*) belongs to a relatively new class of violet organic pigments called 'benzimidazolone dioxazines' (Kaul & Kempter, 1993; Boeglin *et al.*, 1998; Kempter & Wilker, 2001), which are synthesized in a multi-step synthesis, *e.g.* from tetrachlorobenzoquinone and 5-aminobenzimidazolones.

(1*a*): $C_{22}H_{12}Cl_2N_6O_4$, R = R' = CH_3

(1*b*): $C_{23}H_{14}Cl_2N_6O_4$, R = CH_3, R' = C_2H_5

(1*c*): $C_{24}H_{16}Cl_2N_6O_4$, R = R' = C_2H_5

These pigments show an extremely high colour strength. To our knowledge there is no other commercial organic or inorganic pigment with a higher colour strength. The colour strength of (1*a*) and (1*c*) is *ca* 50% higher than that of C.I. Pigment Violet 23, which was previously the pigment with the highest tinting power that was commercially available (Herbst & Hunger, 2004). If one part of (1*a*) is mixed with 100 parts of TiO_2 and dispersed, *e.g.* in a lacquer, the resulting mixture still has a strong violet colour (similar to the colour of the 'Milka®' chocolate papers). The pigments can be used for the coloration of lacquers, paints, plastics and printing inks. Compound (1*c*) is already produced industrially and registered in the Colour Index (C. I.) as 'C. I. Pigment Blue 80'. Compound (1*a*) is currently under development.

Compound (1*a*) is insoluble in all organic solvents. Even in good solvents such as DMSO or *N*-methylpyrrolidone (NMP), the solubility at 473 K is below the detection limit of *ca* 10 p.p.b. When the compound is heated to boiling in DMSO or NMP, and the reagent tube is removed from the flame, the pigment settles out and the solution is almost colourless, despite the high colour strength. The melting point of (1*a*) is far above 600 K and melting results in decomposition. Sublimation is possible at *ca* 620 K and 10^{-3} mbar, but the crystal quality is not improved.

All attempts to obtain the single crystals were unsuccessful.

During the recrystallization attempts we detected six different polymorphic forms exhibiting different reddish-violet to bluish-violet shades (Kempter *et al.*, 2002). In the chemical synthesis of (1*a*) in concentrated H_2SO_4 the δ phase is formed. The β phase can be synthesized by the protonation of (1*a*) with CF_3COOH and subsequent 'dilution' by glacial acetic acid (deprotonation). The ε phase is formed by protonation with CF_3COOH and the subsequent slow evaporation. Analoguously, the ζ phase precipitates from a mixture of CF_3COOH and *o*-dichlorobenzene [CF_3COOH evaporates first causing the pigment to precipitate, because neither (1*a*) nor its protonated form are soluble in *o*-dichlorobenzene]. The α phase is formed by treating one of the other phases with boiling NMP at *ca* 475 K for 18 h. Under high shearing forces (by salt-kneading) with a solvent, the μ phase emerges. The most stable phase thermodynamically seems to be the α phase.

All powder diagrams were of low quality, showing only a few quite broad peaks. The powder diagram of the β phase is shown in Fig. 1. From the line widths (full widths at half maximum of *ca* 0.5° in 2θ) the crystallite size can be estimated to be *ca* 20 nm. The powder diagrams of other polymorphic forms of (1*a*) were of even poorer quality. None of the powder diagrams could be indexed. For the β phase indexing trials with 13 peak positions [at 2θ = 6.51, 11.15, 13.09, 14.49, 19.63, 21.11, 21.43 (shoulder), 22.40, 23.67, 25.34, 27.47, 29.49 and 32.52°] using different indexing programs resulted in various orthorhombic, monoclinic and triclinic unit cells, but it was not possible to determine which would be the correct one. Therefore, the crystal structure had to be solved *a priori*, *i.e.* without any knowledge of the lattice parameters and space group.

2. Experiments and calculations

2.1. Synthesis and recrystallization of $C_{22}H_{12}Cl_2N_6O_4$ (1*a*)

The compound (1*a*) was synthesized by condensation of tetrachlorobenzoquinone (chloranil) with two equivalents of 5-amino-1-methylbenzimidazolone, followed by oxidation and ring closure with MnO_2 in concentrated sulfuric acid, as described by Boeglin *et al.* (1998). The resulting δ phase of (1*a*) was dissolved by protonation in CF_3COOH at room temperature. On slow dilution with glacial acetic acid at room temperature the β phase of (1*a*) precipitated. Finally, the suspension was heated to boiling for 10 min.

2.2. X-ray powder measurements

A powder sample of β-(1*a*) was placed between thin films of biaxially oriented polyethylene terephthalate and measured in transmission mode on a STOE-Stadi-P diffractometer using Cu $K\alpha_1$ radiation. The diffractometer was equipped with a primary-beam Ge [111] monochromator and a linear position-sensitive detector. The total measuring time was *ca* 2 h. The peak widths and background are caused by the poor crystallinity and the small crystal size of the material. A longer exposure time could reduce the statistical noise, but will not increase the information content. The use of synchrotron radiation is not indicated, since the high peak width and the low quality of the data are caused by the poor crystallinity of the sample, not by the diffraction experiment.

2.3. Prediction of possible crystal structures

2.3.1. Molecular geometry. The molecular geometry of (1*a*) was constructed from the single-crystal data of (2) (Dietz & Paulus, 1991) and (3) (Hunger *et al.*, 1982; Paulus, 1997).

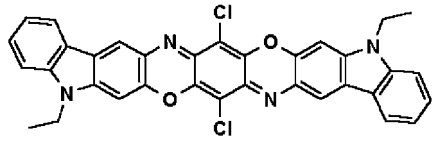

(2)

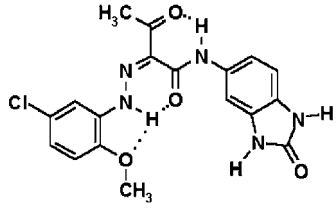

(3)

To confirm the constructed geometry, CSD searches (Cambridge Structural Database, 1999) on fragments were carried out and the molecular geometry was also calculated with the quantum mechanical method AM1. All three methods gave similar results. The molecule (1*a*) was assumed to be planar, as indicated by AM1 and the crystal structures of (2) and similar compounds. The molecule (1*a*) does not possess any intramolecular degree of freedom which could be influenced significantly by crystal packing. (The rotation of the methyl group around the N—CH_3 bond has almost no influence on the crystal structure, thus it could be kept fixed.) Therefore, the molecule was treated as a rigid body in the energy minimization step.

2.3.2. Energy minimizations. The possible crystal structures of (1*a*) were calculated using the program *CRYSCA* ('Crystal Structure Calculations'; Schmidt, 1995; Schmidt & Englert, 1996; Schmidt & Kalkhof, 1999). *CRYSCA* performs global lattice-energy optimizations for rigid or flexible molecules, starting from a set of several thousand random crystal structures with random values for the lattice parameters, and the orientation and position of the molecules. All starting values

Table 1
Parameters for the van der Waals potential (Schmidt, 1995, 1999; Schmidt & Englert, 1996).

Atoms	A (Å^6 kJ mol^{-1})	B (kJ mol^{-1})	C (Å^{-1})	Atoms	A (Å^6 kJ mol^{-1})	B (kJ mol^{-1})	C (Å^{-1})
C···C	2377.0	349908	3.60	H†···H†	0	0	0
C···H	523.0	36677	3.67	H†···H	144.2	11104	3.74
H···H	144.2	11104	3.74	H†···C	523.0	36677	3.67
N···N	1240.7	201191	3.78	H†···N	0	0	0
N···C	1483.6	247571	3.73	H†···O	0	0	0
N···H	407.4	64467	4.00	Cl···Cl	6000.0	1000000	3.56
O···O	1242.6	372203	4.18	Cl···C	3777.0	591530	3.58
O···C	1718.6	360883	3.89	Cl···H	930.2	105376	3.65
O···H	423.3	64288	3.96	Cl···N	2728.0	448543	3.67
O···N	1241.6	273649	3.98	Cl···O	2730.0	610084	3.87
				Cl···H†	930.2	105376	3.65

† H atom of the OH and NH groups.

are limited to user-defined sensible ranges. In the case of flexible molecules the molecular flexibility is also included from the beginning. The crystal symmetry is given as input. In contrast to some other programs, *CRYSCA* is able to handle all space groups and site symmetries (special positions), as well as disorders, noncrystallographic symmetries *etc.*

For (1*a*), the space group was not known in advance. Thus, separate calculations were performed with statistically the most common crystal symmetries ($P2_1/c$, $Z = 4$; $P\bar{1}$, $Z = 2$; $P2_1$, $Z = 2$; $C2/c$, $Z = 8$; $P2_12_12_1$, $Z = 4$ *etc.*; Chernikova *et al.*, 1990; Belsky *et al.*, 1995). The molecular point group of (1*a*) is 2/*m*. From the work of Kitajgorodskij (1970), it is known that most molecules with molecular inversion centres are situated on crystallographic inversion centres in the solid state; this was recently confirmed by Pidcock *et al.* (2003). In contrast, molecular mirror planes or twofold axes are less frequently maintained in the crystal structures. Thus, it was likely that molecule (1*a*) could be situated on a crystallographic inversion centre. Therefore, the energy minimizations were carried out additionally in those crystal symmetries being most frequent for molecules with inversion centres ($P2_1/c$, $Z = 2$; $P\bar{1}$, $Z = 1$; $C2/c$, $Z = 4$). In principle, these additional calculations were not necessary, since all packings with molecules on special positions are found in the calculations in the corresponding subgroups as well, *e.g.* all packings in $P2_1/c$, $Z = 2$, should also be found during the calculations in the subgroups $P2_1$, $Z = 2$ and $P2_1/c$, $Z = 4$. On the other hand, calculations with molecules on special positions require a much shorter calculation time because of the lower number of parameters; therefore, we generally perform such calculations.

In *CRYSCA* the energy is calculated by the formula:

$$E = \frac{1}{2}\sum_i \sum_j \left(-A_{ij} r_{ij}^{-6} + B_{ij}\, e^{-C_{ij} r_{ij}} + \frac{1}{4\pi\varepsilon\varepsilon_0}\frac{q_i q_j}{r_{ij}} \right) + E_{\text{intramol}}, \quad (1)$$

where *i*: all atoms of a reference molecule; *j*: all atoms of all other molecules; r_{ij}: interatomic distance; A, B, C: van der Waals' parameters; q: atomic charges; $\varepsilon = 1$; E_{intramol}: intramolecular energy. E_{intramol} is omitted for (1*a*) since the molecule is rigid.

The values for A, B and C are given in Table 1. These parameters have been shown to work well for various organic and organometallic compounds (Schmidt & Englert, 1996; Schmidt, 1999; Schmidt & Dinnebier, 1999; Lommerse *et al.*, 2000).

Atomic charges were calculated by the charge iteration method based on the Extended Hückel Theory using the program *FORTICON*8 (Howell *et al.*, 1977). Normal EHT calculations are known to give charges which are too high. The EHT charge-iteration procedure had been developed in order to obtain more reliable charges. In this procedure, the diagonal Hamilton matrix elements are given by $H_{ii} = -VSIE(q)$, where $VSIE(q)$ is the valence state ionization energy of orbital i when the atom has the total charge q. The resulting charges are comparable to the Gasteiger charges. With these charges, the molecular dipole moments of a series of small organic and organometallic molecules were reproduced quite well (Schmidt, 1995). For (1*a*), the charges of the N and H atoms of the N—H group were manually set to −0.258 and +0.200 *e*, respectively, because test calculations had shown that these values result in the formation of reliable, linear hydrogen bridges. All charges were multiplied by a factor of 1.1 to scale the electrostatic energy against the van der Waals' energy (Schmidt, 1995; Schmidt & Englert, 1996).

In CRYSCA the lattice energy is minimized by a special steepest-descent algorithm. The total calculation time was of the order of a few weeks of CPU time on a standard single-processor workstation. The minima were sorted according to energy, and manually checked for higher symmetries and reliable intermolecular interactions. All energetically favorable packings with molecules on inversion centres were also found in the corresponding subgroups with molecules in general positions. Most low-energy packings were found more than once (*i.e.* from different starting values), which indicates that all low-energy packings have been found and no energetically favorable minimum is missing. In the case of small simple molecules, the lattice energy minimizations may result in a list of more than a hundred possible crystal structures within an energy range of a few kJ mol^{-1} above the global minimum (Lommerse *et al.*, 2000). In contrast, for molecule (1*a*) we only found seven possible structures within 10 kJ mol^{-1} and 21 structures within 20 kJ mol^{-1}. The pack-

Table 2
Predicted possible crystal structures of (1*a*).

Energy rank	Energy (kJ mol^{-1})	Space group	Z	Site symmetry	a (Å)	b (Å)	c (Å)	α (°)	β (°)	γ (°)	Density (g cm^{-3})
1	−259.7	$P2_1/c$	2	$\bar{1}$	4.383	8.365	26.014	90	102.56	90	1.767
2	−253.2	$C2/c$	4	$\bar{1}$	20.482	8.431	11.635	90	108.96	90	1.731
3	−251.6	$P2_1/c$	4	1	4.421	8.385	51.658	90	93.42	90	1.726
4	−251.1	$P2_1/c$	2	$\bar{1}$	12.923	8.416	8.840	90	98.49	90	1.729
5	−250.7	$P\bar{1}$	1	$\bar{1}$	4.335	8.419	13.906	106.95	92.91	95.12	1.706

ings having the lowest energy are summarized in Table 2. The molecules are connected by hydrogen bonds of the type N—H···O═C, which form either eight-membered rings (Fig. 2*a*) or chains (Fig. 2*b*). From the ten best structures, only one (energy rank 5) shows the ring pattern, one structure (rank 3) contains both patterns and the other eight structures have the chain motif.

For all the possible predicted crystal structures the X-ray powder diagrams were calculated using a Peudo-Voigt function for the peak shape and assuming a crystallite size of 20 nm (to simulate the line broadening). The resulting diagrams were compared with the experimental powder diagram of the β phase of (1*a*) (Fig. 3).

3. Results and discussion

The calculated possible structure with energy rank 5 showed an X-ray powder diagram similar to the experimental powder diagram of the β phase of (1*a*), whereas all the other powder diagrams did not match, especially in the low-angle region (see Fig. 3). It could be concluded that the packing with energy rank 5 corresponds to the correct crystal structure of the β phase. The calculated structure is shown in Fig. 4.

Some of the other simulated diagrams have some similarities with experimental powder diffraction data of other polymorphic forms of (1*a*), but the quality of the experimental powder diagrams was too low to reach any definitive conclusions.

Although the crystal structure of the β phase seemed to be solved, it was difficult to confirm the correctness of the structure. To obtain proof of the crystal structure a Rietveld refinement is usually performed. If the refinement converged with good confidence values, with a smooth difference curve, with an acceptable molecular geometry and sensible intermolecular distances, then the structure would be regarded as successfully determined. However, the powder diagram of (1*a*) contained only about 12 peaks and some shoulders, and hence the information content of the diagram is quite low. We regarded a Rietveld refinement for this triclinic structure as being not very reliable, even if the molecule is described as a rigid body. Thus, we looked for other analytical techniques, which might be able to confirm the crystal structure.

Solid-state NMR investigations (double quantum ^{1}H measurements) were performed to obtain information on the intermolecular H···H distances in (1*a*) (Spieß & Brown, 1999). While the spectra looked promising, the crystal structure could not be finally proved.

Electron diffraction was tried as well (Kolb, 2001). However, the crystal quality was not sufficient and the material was too sensitive to the electron beam to obtain diffraction patterns suitable at least for the determination of the unit-cell parameters.

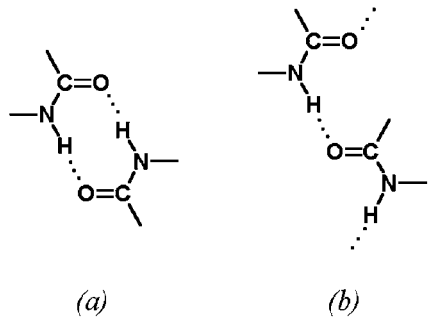

Figure 2
Hydrogen-bond patterns in the predicted crystal structures of (1*a*): (*a*) eight-membered ring; (*b*) zigzag chain.

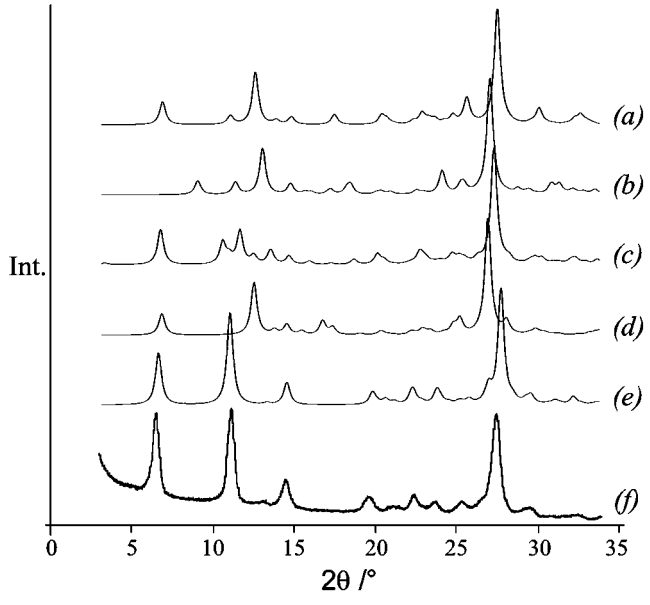

Figure 3
X-ray powder diagrams of (1*a*): (*a*)–(*e*) simulated diagrams of the predicted crystal structures with energy ranks 1–5, respectively, without any fit to the experimental powder diagram. (*f*) Experimental X-ray powder diagram.

Table 3
Experimental details.

	Structure from energy minimization (without any fit to the powder diagram)	Structure from Rietveld refinement
Space group	$P\bar{1}$	$P\bar{1}$
Z	1	1
a (Å)	4.335	4.275 (2)
b (Å)	8.419	8.311 (3)
c (Å)	13.906	14.092 (5)
α (°)	106.95	107.23 (3)
β (°)	92.91	93.53 (2)
γ (°)	95.12	97.17 (3)
V (Å^3)	481.9	472.0 (3)
ρ (g cm^{-3})	1.706	1.74 (1)
λ (Å)		1.54056 (Cu $K\alpha_1$)
2θ range (°)		3–34
R_p (Le Bail)		0.102
R_p		0.225
R_{wp}		0.212
R_{F^2}		0.162
χ^2		11.5
No. of refined parameters	9 (a, b, c, α, β, γ, molecular orientation)	9 (a, b, c, α, β, γ, $B_{overall}$, scale factor, zeropoint)
No. of reflections		109

Table 4
Atomic coordinates of β-(1a) determined by lattice energy minimization (left) and Rietveld refinement (right).

The molecule is situated on an inversion centre at (0,0,0). The second half of the molecule is generated by $-x$, $-y$, $-z$.

	Lattice energy minimization			Rietveld refinement		
	x	y	z	x	y	z
C1	0.06106	−0.13993	0.03139	0.05795	−0.14104	0.03130
C3	0.22942	0.02065	0.08267	0.23043	0.02443	0.08370
C2	0.15438	0.15873	0.04628	0.15843	0.16338	0.04733
O1	0.30602	0.31430	0.09177	0.31404	0.32352	0.09386
C5	0.52628	0.33430	0.17113	0.53528	0.34715	0.17420
C4	0.58923	0.19557	0.20313	0.59515	0.20735	0.20612
N1	0.43699	0.03676	0.15764	0.43886	0.04392	0.15959
Cl1	0.13968	−0.30841	0.07105	0.13283	−0.31079	0.07087
C6	0.67187	0.49282	0.21421	0.68490	0.51019	0.21830
C7	0.89375	0.51295	0.29416	0.90776	0.53398	0.29924
C8	0.96542	0.37770	0.32913	0.97645	0.39784	0.33418
C9	0.81254	0.21988	0.28333	0.81955	0.23540	0.28733
N10	1.19759	0.44472	0.40982	1.21072	0.46936	0.41602
C11	1.26246	0.61657	0.42248	1.27974	0.64470	0.42939
O11	1.45336	0.71473	0.48604	1.47337	0.74718	0.49401
N2	1.07457	0.65643	0.35111	1.09234	0.68229	0.35732
C16	1.07205	0.82180	0.33951	1.09366	0.85003	0.34613
H6	0.61942	0.59240	0.18858	0.63464	0.61043	0.19270
H9	0.86409	0.11987	0.30866	0.86889	0.13472	0.31263
H10	1.30181	0.38234	0.45200	1.31373	0.40765	0.45849
H161	1.08264	0.90885	0.41051	1.10320	0.93834	0.41628
H162	0.87597	0.82358	0.29368	0.89605	0.84880	0.29907
H163	1.26595	0.84749	0.30325	1.29311	0.87929	0.31237

Finally, we have tried a Rietveld refinement using the program *Fullprof* (Rodriguez-Carjaval, 1990; Fig. 5). The molecule was treated as rigid. The data quality was only sufficient to refine the lattice parameters, scale factor, $B_{overall}$ and zeropoint (Table 3). The spatial orientation of the molecule had to be calculated by lattice energy minimization runs between the Rietveld steps. The position of the molecule [on an inversion centre at (0,0,0)] could be kept fixed. The refinements converged, but the R values were quite high and the difference curve is not fully convincing (see Fig. 6). Furthermore, during the refinements the molecules came closer together, causing a distortion of the intermolecular hydrogen bonds (see Fig. 5). From the chemical point of view the refined structure is less sensible than the structure calculated by lattice energy minimization. Although the Rietveld refinements seemed to confirm the crystal structure, this could

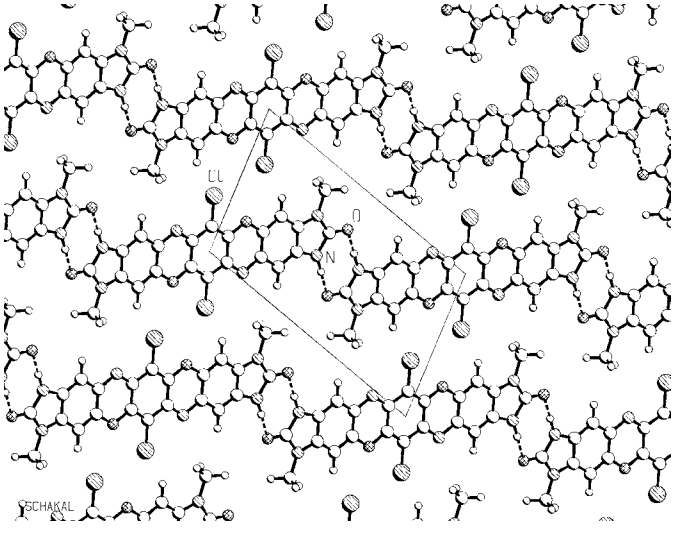

Figure 4
Crystal structure of β-(1a) calculated by lattice energy minimizations (energy rank 5) without any fit to the experimental X-ray powder diagram. *SCHAKAL* plot (Keller, 1999). View direction [100].

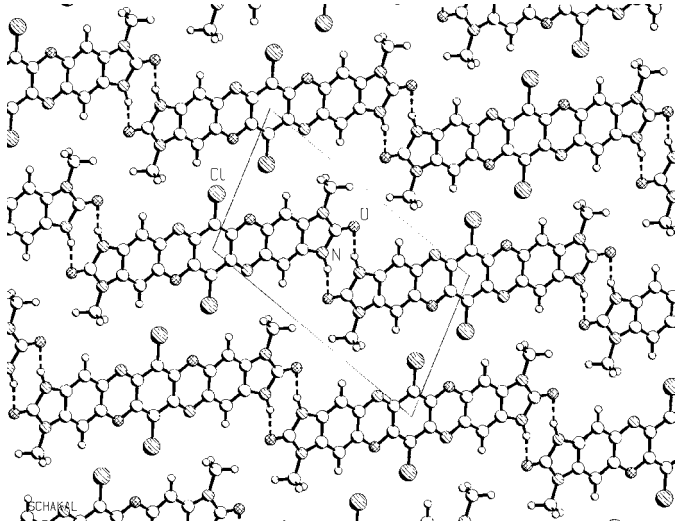

Figure 5
Refined crystal structure of β-(1a) (constrained Rietveld refinement). View direction [100].

not be regarded as definite proof. Table 4 contains the calculated as well as the refined atomic coordinates.

An evaluation of the unit cells proposed by the indexing trials revealed that none of these unit cells correspond to the experimental cell. The reason might be that the peak positions could not be determined with a suffiently high accuracy.

The crystal structure of (1*a*) consists of layers built from chains of molecules. The molecules are connected by hydrogen bridges of the type N—H···O═C forming eight-membered rings (Fig. 2*a*). This binding pattern has also been found in several other *cis*-amide systems. In contrast, other patterns such as zigzag chains (Fig. 2*b*) are also known (*e.g.* Allen *et al.*, 1999).

The molecular packing of (1*a*) is quite efficient and the density is quite high for an organic compound (ρ_{CRYSCA} = 1.706, $\rho_{\rm Rietveld}$ = 1.74 g cm^{-3}). Also the rule of thumb which states '18 Å^3 per non-hydrogen atom' (Kempster & Lipson, 1972) does not hold (*CRYSCA*: 14.17 Å^3, Rietveld: 13.88 Å^3). This high packing density is one reason for the observed insolubility of (1*a*). Another reason is the simultaneous occurrence of the hydrogen bridges (which cannot be broken by aprotic solvents) and of the strong van der Waals forces (which cannot be broken by water or protic solvents). On the other hand, there is still a small space between the methyl groups of neighbouring molecules so the packing of the β phase is not the optimal one. This is probably the reason for the existence of more than one polymorphic form.

If the space between the methyl groups was filled, the crystal structure would be even more dense. For pigments, high packing efficiencies generally result in good application properties. Thus, 'crystal engineering' can be applied, *i.e.* based on the knowledge of the crystal structure it is possible to perform targeted synthesis to obtain materials with improved solid-state properties. A thorough inspection of the crystal structures of (1*a*) by *CRYSCA* revealed that the space between the methyl groups is large enough for one additional CH_2 group, *i.e.* the substitution of one methyl group by an ethyl group. The space is not sufficient for both methyl groups being replaced by ethyl groups; if two ethyl groups were present, at least one of them would stick out of the plane. [This is indeed the case, as the crystal structure of (1*c*) with two ethyl groups shows; Schmidt & Dinnebier, 2005.]

Hence, the compound (1*b*) having R = CH_3, R' = C_2H_5, would be the optimum choice. This compound is difficult to synthesize in a pure form. Rather than just (1*b*), a mixed crystal (solid solution) consisting of [(1*a*) + (1*b*) + (1*c*)] (approximate ratio 1:2:1) was investigated. Such mixed crystals were formed when the synthesis was carried out with a mixture of the methyl and ethyl derivatives of 5-aminobenzimidazolone (Schmidt *et al.*, 2002). The powder diagrams of [(1*a*) + (1*b*) + (1*c*)] indicate that this mixed crystal exists in two different polymorphic forms, which are isostructural to the β and δ phases of (1*a*): The δ phase of the mixed crystal is formed in the synthesis step and shows a powder diagram consisting of only a few very broad lines. By heating the δ phase in *N*-methylpyrrolidone at 475 K, the mixed crystal transforms into the β phase. Such transformations between different polymorphic forms of a mixed crystal without any change in the chemical composition are well known in inorganic chemistry, but rarely described for organic compounds.

Generally, mixed crystals (solid solutions) of organic compounds tend to show X-ray powder diagrams which are not as well resolved as their parent compounds, since the different sizes of the molecules result in a higher number of lattice defects and hence in line broadening. To our great surprise, the X-ray powder diagram of the β phase of [(1*a*) + (1*b*) + (1*c*)] was of much better quality than we had ever observed for any phase of (1*a*) (see Fig. 7). The diagram could be indexed unambiguously, using the program *ITO* (Visser, 1969) inside the *WinXPOW* package (STOE, 2000). The lattice parameters were quite similar to those for (1*a*). The structure of (1*a*) was used as a starting point for the Rietveld refinements of [(1*a*) + (1*b*) + (1*c*)] (Schmidt & Dinnebier, 2005). The refinement converged well and lead to a crystal structure very similar to the structure of β-(1*a*), thereby proving that our previously determined crystal structure of β-(1*a*) was correct.

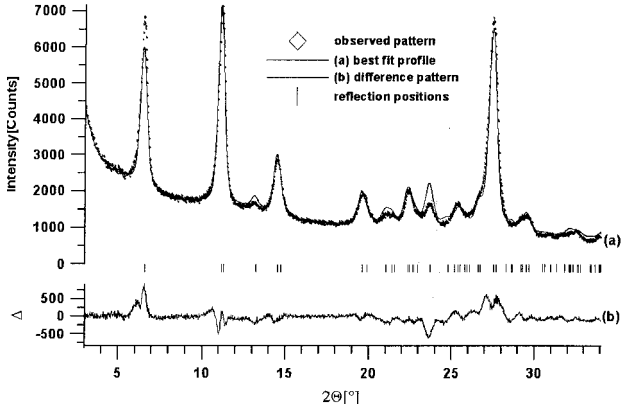

Figure 6
Constrained Rietveld refinement of (1*a*).

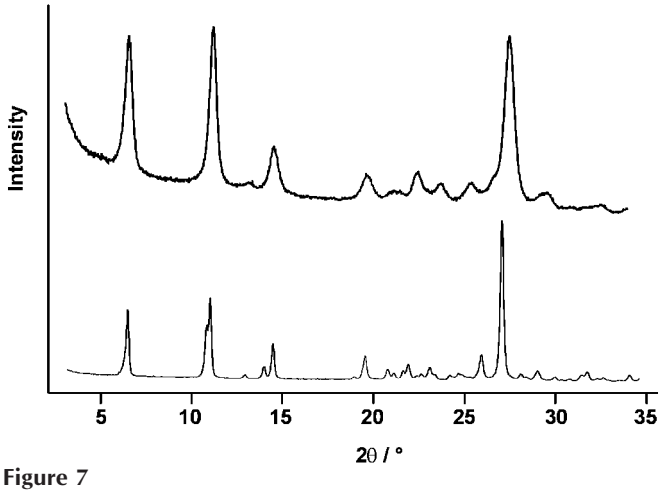

Figure 7
Powder diagrams of the β phase of (1*a*) (top) and of the solid solution of [(1*a*) + (1*b*) + (1*c*)] (bottom).

4. Conclusions

The structure determination of β-(1*a*) from a non-indexed low-quality X-ray powder diagram shows that the structures of molecular compounds may be solved by lattice energy minimization from diffraction data with limited quality, even when indexing is not possible.

The limitations of the method are:

(i) Compounds of unknown composition.

(ii) Powder diagrams with less than 10–15 peaks [since it is no longer possible to select the correct structure from the list of calculated possible structures. The diagram of β-(1*a*) having 12 visible peaks was already at the limit].

(iii) Unexpected crystal symmetries (which are not considered in the energy minimization, unless there is a hint for them).

(iv) Missing or unsuitable force-field terms.

(v) Solvates, hydrates and structures with more than one molecule per asymmetric unit. There are examples of correct crystal structure predictions with $Z' = 2$ (see *e.g.* Bayer *et al.*, 2001; van Eijck, 2002; Motherwell *et al.*, 2005), but the calculation time increases exponentially with the number of parameters to be determined.

(vi) Ionic molecular crystals have rarely been calculated, because of force-field problems. First successful examples have been carried out by van de Streek (2005) and McArdle *et al.* (2004).

If the powder is of very low crystallinity and the X-ray powder diagram shows less than 10–15 visible peaks, the crystal structure may only be solved if additional assumptions are made, *e.g.* on the lattice parameters or on the packing (see *e.g.* Masciocchi *et al.*, 2002).

The accuracy of a crystal structure determined from limited-quality powder data is lower than the accuracy of a single-crystal structure determination. Nevertheless, the packing of the molecules is determined and the knowledge of the crystal structure can be used for structure–property relationships and crystal engineering.

The authors wish to thank Dr Peter Kempter (Clariant GmbH) for the syntheses, Dr Holger Kalkhof (Clariant GmbH, now at Jerini, Berlin), for the programming, Professor Dr Erich F. Paulus (former Hoechst AG, now Frankfurt University) and Mrs Ursula Conrad (former Hoechst AG) for the X-ray powder measurements of (1*a*), and the pigments research group of Clariant GmbH (Dr Hans-Joachim Metz and Dr Carlsten Plüg) for the cooperation and financial support. Finianclal support by the Bundesministerium für Bilding und Forschung (BMBF) and the Fonds der Chemischen Industrie (FCI) is gratefully acknowledged.

References

Allen, F. H., Motherwell, W. D. S., Raithby, P. R., Shields, G. P. & Taylor, R. (1999). *New J. Chem.*, pp. 25–34.

Altomare, A., Burla, M. C., Camalli, M., Carrozzini, B., Cascarano, G. L., Giacovazzo, C., Guagliardi, A., Moliterni, A. C. G., Polidori, G. & Rizzi, R. (1999). *J. Appl. Cryst.* **32**, 339–340.

Bayer, T., Lewis, T. & Price, S. L. (2001). *CrystEngComm.* **44**, 1–27.

Belsky, V. K., Zorkaya, O. N. & Zorky, P. M. (1995). *Acta Cryst.* A**51**, 473–81.

Boeglin, P., Kaul, B. L. & Kempter, P. (1998). European Patent EP 0 911 337 A1.

Bond, A. D. & Jones, W. (2002). *Acta Cryst.* B**58**, 233–243.

Cambridge Structural Database (1999). Cambridge Crystallographic Data Centre, 12 Union Road, Cambridge, England.

Cascarano, G., Favia, L. & Giacovazzo, C. (1992). *J. Appl. Cryst.* **25**, 310–317.

Chan, F. C., Anwar, J., Cernik, R., Barnes, P. & Wilson, R. M. (1999). *J. Appl. Cryst.* **32**, 436–441.

Chernikova, N. Yu., Belsky, V. K. & Zorky, P. M. (1990). *Zh. Strukt. Khim.* **31**, 148–153.

Chernyshev, V. V. & Schenk, H. (1998). *Z. Kristallogr.* **213**, 1–3.

Cheung, E. Y., McCabe, E. E., Harris, K. D. M., Johnston, R. L., Tedesco, E., Raja, K. M. P. & Balaram, P. P. (2002). *Angew. Chem.* **114**, 512–514.

David, W. I. F., Shankland, K. & Shankland, N. (1998). *Chem. Commun.* pp. 931–932.

Dietz, E. & Paulus, E. F. (1991). Presentation on the Farbensymposium, Montreux.

Dinnebier, R. E., Sieger, P., Nar, H., Shankland, K. & David, W. I. F. (2000). *J. Pharm. Sci.* **89**, 1465–1479.

Dorset, D. L. (1996). *Acta Cryst.* B**52**, 753–769.

Eijck, B. P. van (2002). *J. Comput. Chem.* **23**, 456–462.

Engel, G. E., Wilke, S., König, O., Harris, K. D. M. & Leusen, F. J. J. (1999). *J. Appl. Cryst.* **32**, 1169–1179.

Erk, P. (2002). *High Performance Pigments*, edited by H. M. Smith, pp. 103–123. Weinheim: Wiley-VCh.

Fagan, P. G., Hammond, R. B., Roberts, K. J., Docherty, R., Chorlton, A. P., Jones, W. & Potts, G. D. (1995). *Chem. Mater.* **7**, 2322–2326.

Gavezzotti, A. & Filippini, G. (1996). *J. Am. Chem. Soc.* **118**, 7153–7157.

Hammond, R. B., Roberts, K. J., Docherty, R., Edmondson, M. & Gairns, R. (1996). *J. Chem. Soc. Perkin Trans. 2*, pp. 1527–1528.

Harris, K. D. M. & Tremayne, M. (1996). *Chem. Mater.* **8**, 2554–2570.

Harris, K. D. M., Tremayne, M. & Kariuki, B. M. (2001). *Angew. Chem.* **113**, 1674–1700.

Herbst, W. & Hunger, K. (2004). *Industrial Organic Pigments*, 3rd ed. Weinheim: Wiley-VCH.

Howell, J., Rossi, A., Wallace, D., Haraki, K. & Hoffmann, R. (1977). *ICON*, FORTICON Version 8, QCPE program No. 517. Quantum Chemical Programs Exchange 11, p. 344.

Hunger, K., Paulus, E. F. & Weber, D. (1982). *Farbe Lack*, **88**, 453–458.

Kaul, B. L. & Kempter, P. (1993). German Patent DE 44 42 291 A1.

Keller, E. (1999). *SCHAKAL*99. Kristallographisches Institut der Universität Freiburg, Freiburg, Germany.

Kempster, C. J. E. & Lipson, H. (1972). *Acta Cryst.* B**28**, 3674.

Kempter, P. & Wilker, G. (2001). *Farbe Lack*, **107**, 29–31.

Kempter, P., Schmidt, M. U. & Born, R. (2002). European Patent EP 1199309 A1.

Kitajgorodskij, A. I. (1970). *Adv. Struct. Res. Diffr. Methods* **3**, 179–247.

Kolb, U. (2001). Unpublished results.

Kolb, U. & Matveeva, G. N. (2003). *Z. Kristallogr.* **218**, 1–10.

Lasocha, W., Czapkiewicz, J., Milart, P. & Schenk, H. (2001). *Z. Kristallogr.* **216**, 291–294.

Lommerse, J. P. M., Motherwell, W. D. S., Ammon, H. L., Dunitz, J. D., Gavezzotti, A., Hofmann, D. W. M., Leusen, F. J. J., Mooij, W. T. M., Price, S. L., Schweizer, B., Schmidt, M. U., van Eijck, B. P., Verwer, P. & Williams, D. E. (2000). *Acta Cryst.* B**56**, 697–714.

Louër, D., Louër, M., Dzyabchenko, V. A., Agafonov, V. & Ceolin, R. (1995). *Acta Cryst.* B**51**, 182–187.

MacLean, E. J., Tremayne, M., Kariuki, B. M., Harris, K. D. M., Iqbal, A. F. M. & Hao, Z. (2000). *J. Chem. Soc. Perkin Trans. 2*, pp. 1513–1519.
Masciocchi, N., Sironi, A., Chardon-Noblat, S. & Deronzier, A. (2002). *Organometallics*, **21**, 4009–4012.
McArdle, P., Gilligan, K., Cunningham, D., Dark, R. & Mahon, M. (2004). *CrystEngComm* **6**, 303–309.
Motherwell, W. D. S., Ammon, H. L., Dunitz, J. D., Dzyabchenko, A., Erk, P., Gavezzotti, A., Hofmann, D. W. M., Leusen, F. J. J., Lommerse, J. P. M., Mooij, W. T. M., Price, S. L., Scheraga, H., Schweizer, B., Schmidt, M. U., van Eijck, B. P., Verwer, P. & Williams, D. E. (2002). *Acta Cryst.* B**58**, 647–661.
Motherwell, W. D. S., Day, G., Ammon, H. L., Boerrigter, S., Della Valle, R., Dunitz, J. D., Dzyabchenko, A., van Eijck, B. P., Erk, P., Facelli, J., Gavezzotti, A., Hofmann, D. W. M., Leusen, F. J. J., Liang, C., Price, S. L., Scheraga, H., Schweizer, B., Schmidt, M. U., Verwer, P. *et al.* (2005). In preparation.
Paulus, E. F. (1997). Personal communication.
Pidcock, E., Motherwell, W. D. & Cole, J. C. (2003). *Acta Cryst.* B**59**, 634–640.
Putz, H., Schön, J. C. & Jansen, M. (1999). *J. Appl. Cryst.* **32**, 864–870.
Reck, G., Kretschmer, R. G., Kutschabsky, L. & Pritzkow, W. (1988). *Acta Cryst.* A**44**, 417–421.
Rietveld, H. M. (1967). *Acta Cryst.* **22**, 151–152.
Rietveld, H. M. (1969). *J. Appl. Cryst.* **2**, 65–71.
Rodriguez-Carjaval, J. (1990). VX Congress of the IUCr, Satellite Meeting on Powder Diffraction, Toulouse. Abstracts, p. 127.
Schmidt, M. U. (1995). *Kristallstrukturberechnungen metallorganischer Molekülverbindungen.* Verlag Shaker: Technical University of Aachen, Germany. ISBN 3-8265-0588-3.
Schmidt, M. U. (1999). *Crystal Engineering: From Molecules and Crystals to Materials*, edited by D. Braga, F. Grepioni & A. G. Orpen, pp. 331–348. Dordrecht: Kluwer Academic Publishers.
Schmidt, M. U. & Dinnebier, R. E. (1999). *J. Appl. Cryst.* **32**, 178–186.
Schmidt, M. U. & Dinnebier, R. E. (2005). In preparation.
Schmidt, M. U. & Englert, U. (1996). *J. Chem. Soc. Dalton Trans.* pp. 2077–2082.
Schmidt, M. U. & Kalkhof, H. (1999). *CRYSCA*. Clariant GmbH, Pigments Research, Frankfurt am Main, Germany.
Schmidt, M. U., Kempter, P., Plüg, C. & Born R. (2002). European Patent EP 1201718 A1.
Shirley, R. (1980). *Accuracy in Powder Diffraction*, edited by S. Block & C. R. Hubbard, NBS Special Publication 567, pp. 361–382. Darmstadt: STOE. See also http://www.ccp14.ac.uk/.
Spieß, H. & Brown, S. P. (1999). Unpublished results.
STOE (2000). *WinXPOW*, Version 1.07. STOE, Darmstadt, Germany.
Streek, J. van de (2005). In preparation.
Verwer, P. & Leusen, F. J. J. (1998). *Rev. Comput. Chem.* **12**, 327–365.
Visser, J. W. (1969). *J. Appl. Cryst.* **2**, 89–95.
Voigt-Martin, I. G., Li, G., Kolb, U., Kothe, H., Yakimanski, A. V., Tenkovtsev, A. V. & Gilmore, C. (1999). *Phys. Rev. B*, **59**, 6722–6735.
Wagner, K., Hirschler, J. & Egert, E. (2001). *Z. Kristallogr.* **216**, 565–572.